

Electronic structure of clean and Ag-covered single-crystalline $\text{Bi}_2\text{Sr}_2\text{CuO}_6$

P. A. P. Lindberg, Z.-X. Shen, and B. O. Wells

Stanford Electronics Laboratories, Stanford University, Stanford, California 94305

D. B. Mitzi

Department of Applied Physics, Stanford University, Stanford, California 94305

I. Lindau and W. E. Spicer

Stanford Electronics Laboratories, Stanford University, Stanford, California 94305

A. Kapitulnik

Department of Applied Physics, Stanford University, Stanford, California 94305

(Received 5 June 1989)

Photoemission studies of single-crystalline samples of $\text{Bi}_2\text{Sr}_2\text{CuO}_6$ show clear resemblance to the corresponding data for single crystals of $\text{Bi}_2\text{Sr}_2\text{CaCu}_2\text{O}_8$. In particular, a sharp Fermi-level cutoff, giving evidence of metallic conductivity at room temperature, as well as single-component O 1s emission and Cu 2p satellites with a strength amounting to about 50% of that of the main Cu 2p line, are observed. An analysis of the relative core-level photoemission intensities shows that the preferential cleavage plane of single-crystalline $\text{Bi}_2\text{Sr}_2\text{CuO}_6$ is between adjacent Bi-O layers. Deposition of Ag adatoms causes only weak reaction with the Bi and O ions of the $\text{Bi}_2\text{Sr}_2\text{CuO}_6$ substrate, while the Cu states rapidly react with the Ag adatoms, as monitored by a continuous reduction of the Cu 2p satellite intensity as the Ag overlayer becomes thicker.

Among the Cu-O based high-temperature superconductors, the $\text{Bi}_2\text{Sr}_2(\text{CuO}_2\text{Ca})_n\text{CuO}_6$ ($n=0,1,2,\dots$) systems have received much attention. This interest is partly due to the high transition temperatures achieved for $n=1$ and 2, for which transition temperatures around 90 and 110 K have been reported, and partly to the ease with which large single crystals of primarily $\text{Bi}_2\text{Sr}_2\text{CaCu}_2\text{O}_8$ can be made. As a result, to date most of the experimental investigations have been directed towards the $\text{Bi}_2\text{Sr}_2\text{CaCu}_2\text{O}_8$ material, for which a wealth of information is available in the literature.¹

An interesting characteristic of the $\text{Bi}_2\text{Sr}_2(\text{CuO}_2\text{Ca})_n\text{CuO}_6$ ($n=0,1,2,\dots$) systems is the apparent direct correlation between the number of layers and the superconducting properties. Indeed, the transition temperature increases monotonically as the number of (CuO_2Ca) layers increases from zero to one and two.² Therefore, of special interest is to explore the structural and electronic properties of the $\text{Bi}_2\text{Sr}_2(\text{CuO}_2\text{Ca})_n\text{CuO}_6$ ($n=0,1,2,\dots$) systems for different numbers of (CuO_2Ca) layers.

In this paper, we have employed photoemission spectroscopy (PES) in both the ultraviolet (UPS) and the x-ray (XPS) photon energy ranges to study the surface electronic structure of clean and Ag-covered single crystalline $\text{Bi}_2\text{Sr}_2\text{CuO}_6$. Both the UPS and the XPS spectra show strong similarities to the corresponding data for single crystals of $\text{Bi}_2\text{Sr}_2\text{CaCu}_2\text{O}_8$. In particular, an appreciable density of states immediately below the Fermi energy, giving rise to a well-defined Fermi level cutoff, is clearly observed. In addition, as for the $\text{Bi}_2\text{Sr}_2\text{CaCu}_2\text{O}_8$

material, a single O 1s peak is observed and a Cu 2p satellite to main line intensity ratio of 0.5 is determined from the XPS data. An intensity analysis of the various core-level spectra in comparison with the predictions of a theoretical model shows that also single crystals of $\text{Bi}_2\text{Sr}_2\text{CuO}_6$ preferentially cleave between the Bi-O layers. Overlayers of Ag show only weak reaction with the Bi and O states of the $\text{Bi}_2\text{Sr}_2\text{CuO}_6$ substrate, while the Cu states display an appreciable degree of reaction, as is evident from the monotonic loss of intensity of the Cu 2p satellites as the Ag overlayer becomes progressively thicker.

The photoemission experiments were carried out in a Varian photoemission chamber, operating at a pressure of less than 1×10^{-10} Torr. A He discharge lamp and a Mg x-ray source provided photons with energies 40.8 and 1253.6 eV, respectively, while a cylindrical mirror analyzer (CMA) was used to detect the energy distribution of the photoemitted electrons. Ag deposition was performed using a carefully outgassed Ag bead. A transfer arm directly attached to the photoemission chamber allowed for easy replacement of samples without breaking vacuum. The single crystals were transferred into the photoemission chamber and then fractured *in situ*. The preparation of these crystals is described elsewhere.³ X-ray diffraction showed evidence of a single phase, the composition of which was determined using microprobe analysis to be $\text{Bi}_{2.1}\text{Sr}_{1.8}\text{Cu}_{1.1}\text{O}_6$. Magnetic-susceptibility measurements showed that the samples were nonsuperconducting.

Figure 1 shows the valence-band spectrum of a single

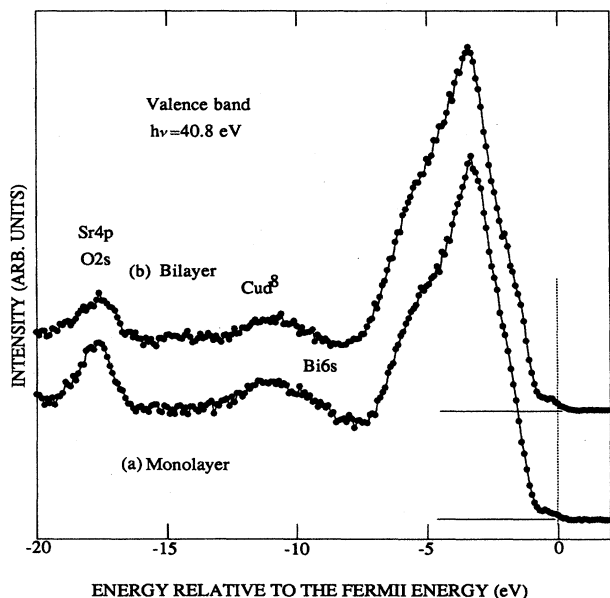


FIG. 1. Comparison of valence-band photoemission spectra using 40.8-eV radiation for (a) $\text{Bi}_2\text{Sr}_2\text{CuO}_6$ and (b) $\text{Bi}_2\text{Sr}_2\text{CaCu}_2\text{O}_8$. Note the different line shapes of the features around -4 and -18 eV. Both compounds show a clear Fermi-level cutoff at room temperature.

crystal of $\text{Bi}_2\text{Sr}_2\text{CuO}_6$ (monolayer) [part (a)] using 40.8-eV radiation, in comparison with the corresponding spectrum recorded from a single crystal of $\text{Bi}_2\text{Sr}_2\text{CaCu}_2\text{O}_8$ (bilayer) [part (b)]. In both compounds a clear Fermi-level cutoff, defining the energy reference level, is observed. As compared to the strength of the main valence-band peaks between -3 and -4 eV, the emission intensity immediately below the Fermi level is slightly larger in $\text{Bi}_2\text{Sr}_2\text{CaCu}_2\text{O}_8$, in qualitative agreement with their results of a previous photoemission study of polycrystalline samples of $\text{Bi}_2\text{Sr}_2\text{CuO}_6$ and $\text{Bi}_2\text{Sr}_2\text{CaCu}_2\text{O}_8$.⁴ Thus, at room temperature both compounds show evidence of metallic conductivity. At higher binding energies, some significant differences in the photoemission spectra from the two compounds are apparent. In the valence-band region, between -7 and -2 eV, the line shape is slightly different. In $\text{Bi}_2\text{Sr}_2\text{CuO}_6$, the shoulder at ~ -5 eV is more clearly discernible, while in $\text{Bi}_2\text{Sr}_2\text{CaCu}_2\text{O}_8$ the emission between -2 eV and the Fermi level appears to be somewhat larger. At energies between -13 and -8 eV, emission due to a $\text{Cu } d^8$ satellite and $\text{Bi } 6s$ states is visible for both compounds. The peak between -17 and -19 eV, which originates from $\text{Sr } 4p$ and $\text{O } 2s$ initial states, is obviously more intense in $\text{Bi}_2\text{Sr}_2\text{CuO}_6$. Hence, since the relative Sr content is larger in $\text{Bi}_2\text{Sr}_2\text{CuO}_6$ than in $\text{Bi}_2\text{Sr}_2\text{CaCu}_2\text{O}_8$, the increased strength of the feature centered at -18 eV points towards $\text{Sr } 4p$ as its main origin, although it is possible that $\text{O } 2s$ states also contribute to the photoemission intensity in this binding energy range.

In Fig. 2, we present core-level photoemission spectra utilizing $\text{Mg } K\alpha$ (1253.6 eV) radiation for selected core

levels of $\text{Bi}_2\text{Sr}_2\text{CuO}_6$: part (a) $\text{Bi } 4f$, part (b) $\text{O } 1s$, part (c) $\text{Sr } 3d$, and part (d) $\text{Cu } 2p_{3/2}$. The spectra in Fig. 2 are in overall agreement with the corresponding spectra previously recorded from single-crystalline $\text{Bi}_2\text{Sr}_2\text{CaCu}_2\text{O}_8$. The energy positions of the $\text{Bi } 4f_{7/2}$, $\text{O } 1s$, $\text{Sr } 3d_{5/2}$, and $\text{Cu } 2p_{3/2}$ core levels are -158.5 , -528.8 , -132.3 , and -933.1 eV, respectively, in good agreement with the results from similar studies of single crystals of $\text{Bi}_2\text{Sr}_2\text{CaCu}_2\text{O}_8$.⁵⁻⁸ Furthermore, the absence of multiple-component $\text{O } 1s$ emission, similar to the $\text{Bi}_2\text{Sr}_2\text{CaCu}_2\text{O}_8$ case, gives evidence of the surface cleanliness. We also note prominent $\text{Cu } 2p$ satellite emission [Fig. 2(d)], giving a satellite to main line intensity ratio of approximately 0.5, consistent with results from single-crystalline $\text{Bi}_2\text{Sr}_2\text{CaCu}_2\text{O}_8$.⁵ However, it is important to note that since the relative Bi content is larger in $\text{Bi}_2\text{Sr}_2\text{CuO}_6$ than in $\text{Bi}_2\text{Sr}_2\text{CaCu}_2\text{O}_8$, the $\text{Bi } 4s$ signal, which appears in the same energy region as the satellite, possibly overestimates the relative strength of the copper satellite in $\text{Bi}_2\text{Sr}_2\text{CuO}_6$ as compared to $\text{Bi}_2\text{Sr}_2\text{CaCu}_2\text{O}_8$.

To extract more information from the core-level photoemission spectra presented in Fig. 2, an intensity analysis was performed based on a model previously described.⁹ This model, which is generally applicable to single-crystalline materials, allows an indirect comparison between the relative photoemission intensities, corrected for transmission characteristics of the analyzer, nominal composition, and photoionization cross section, and estimated (theoretical) relative photoemission intensities based on an assumed crystal model and with corrections made for the mean free paths of the photoemitted electrons. Using this approach, and assuming that the single crystals of $\text{Bi}_2\text{Sr}_2\text{CuO}_6$ are terminated by the Bi-O layer, as in the case of $\text{Bi}_2\text{Sr}_2\text{CaCu}_2\text{O}_8$, we can indirectly relate the structural properties to the electronic structure, as summarized in Table I. Note that all intensities are normalized to the $\text{O } 1s$ signal that has been given the value 100. It is clear from Table I that all deviations between experiment and theory are within $\pm 10\%$, thus supporting the model used. The overall agreement between experiment and theory firmly suggests that the preferential plane of cleavage occurs between two adjacent Bi-O layers, as in the case of $\text{Bi}_2\text{Sr}_2\text{CaCu}_2\text{O}_8$.¹⁰⁻¹³ Furthermore, it is particularly encouraging to note that the intensity ra-

TABLE I. Comparison of experimental relative core-level photoemission intensities corrected for the transmission characteristics of the analyzer, the nominal composition ($\text{Bi}_{2.1}\text{Sr}_{1.8}\text{Cu}_{1.1}\text{O}_6$), and the photoionization cross section [$I_{\text{cor}}(\text{expt})$], with a theoretical model taking account of both the lattice geometry and the mean free path of the photoelectrons (I_{theory}) (Ref. 9). For comparison the $\text{O } 1s$ signal has been normalized to 100.

Core level	$I_{\text{cor}}(\text{expt})$	I_{theory}
$\text{Bi } 4f$	63	63
$\text{Cu } 2p$	9.0	8.1
$\text{Sr } 3d$	59	62
$\text{O } 1s$	100	100

tios of the O 1s signal, to those of the other elements, compare favorably to the theoretical predictions. Thus, the oxygen states appear to be rather stable in ultrahigh vacuum conditions. The small discrepancy in the Sr and Cu signals may be due to substitutional disorder or preferential surface segregation of some of the elements.

To further explore the surface properties and chemistry of the $\text{Bi}_2\text{Sr}_2\text{CuO}_6$ material, photoemission spectra using 1253.6-eV radiation were recorded after deposition of Ag for a number of coverages, as illustrated in Fig. 3,

which shows the evolution of the valence band [part (a)], and the Bi 4*f* [part (b)], O 1s [part (c)], and Cu 2*p*_{3/2} core levels for progressively larger Ag coverages. The effects of the Ag adatoms are perhaps most easily observed in the valence-band spectra which dramatically change character between -8 and -1 eV, as the Ag 4*d* states around -5 eV start to dominate the emission in the valence-band spectrum. As a result, the relative intensity of the Sr 4*p*/O 2*s* states between -20 and -17 eV, the Cu *d*⁸ satellite and Bi 6*s* states between -12 and -9 eV,

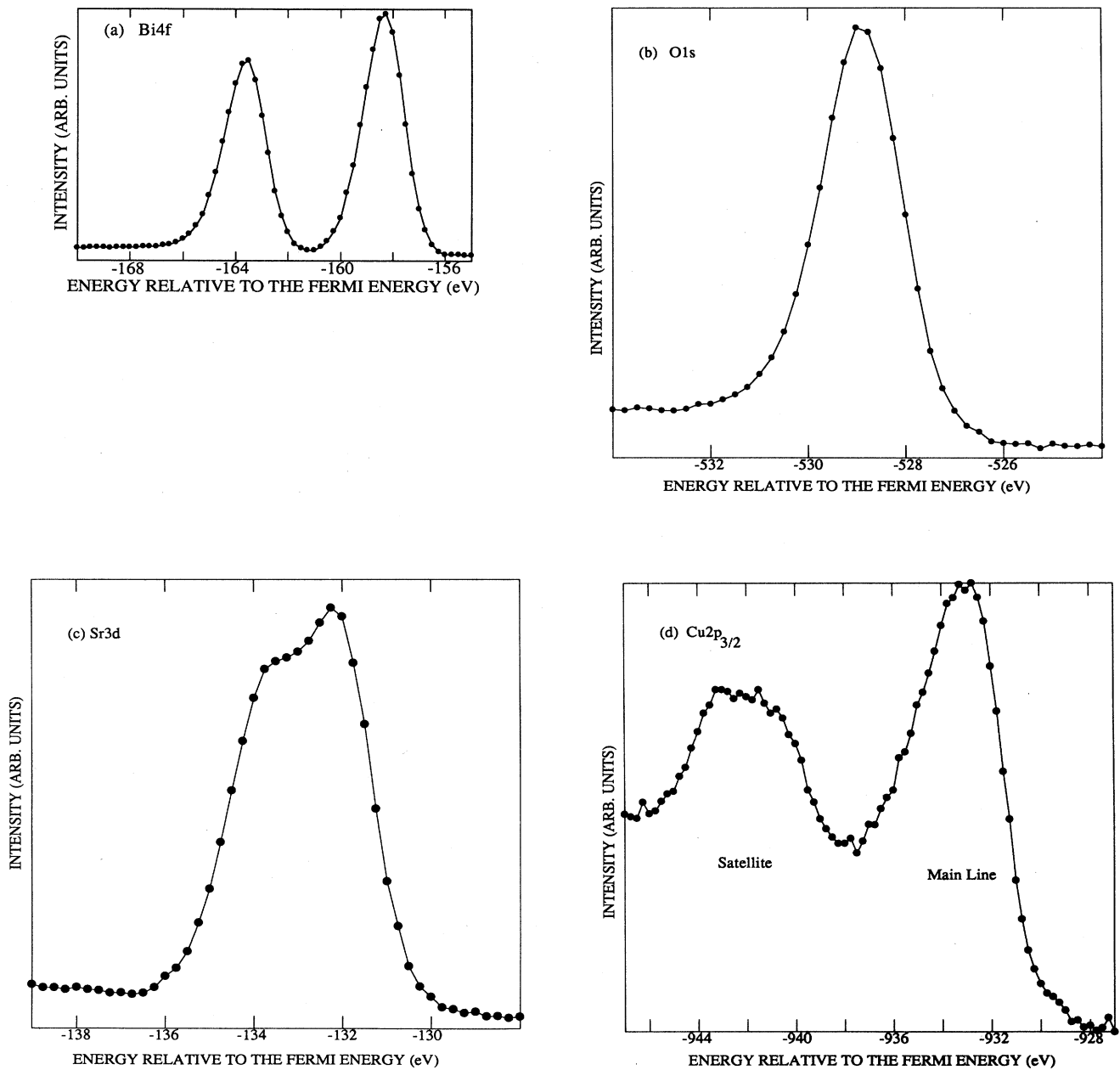


FIG. 2. Photoemission spectra showing selected core levels of $\text{Bi}_2\text{Sr}_2\text{CuO}_6$ using 1253.6-eV radiation: (a) Bi 4*f*, (b) O 1s, (c) Sr 3*d*, and (d) Cu 2*p*.

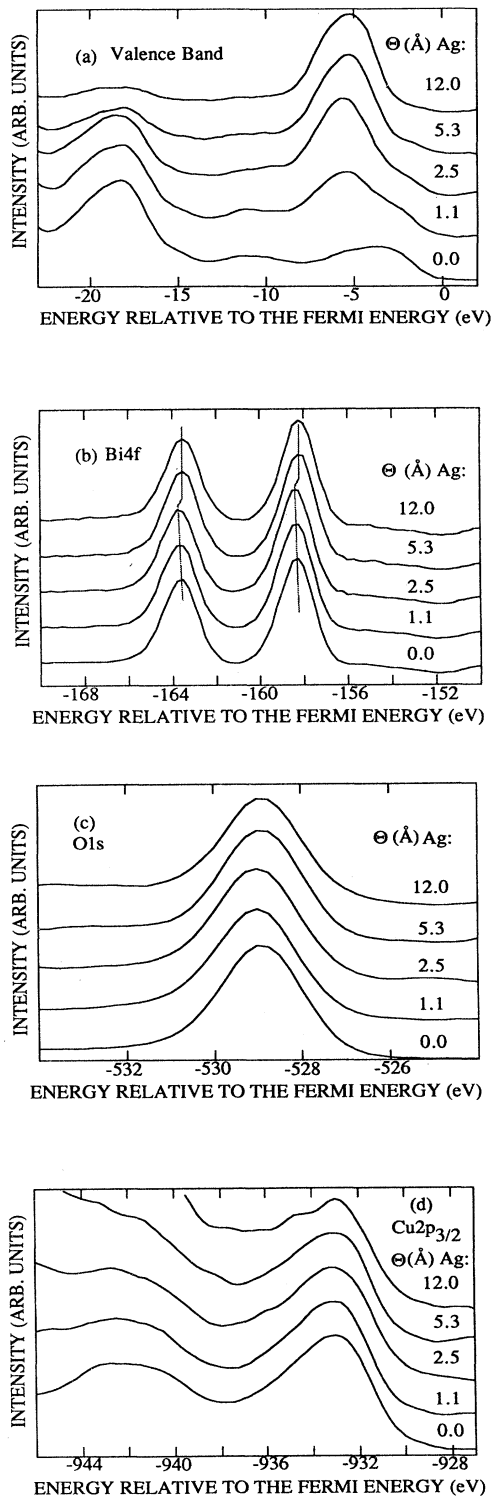


FIG. 3. The evolution of the valence band and selected core levels of $\text{Bi}_2\text{Sr}_2\text{CuO}_6$ as a function of Ag coverage. The various figures show the valence-band [part (a)], and the Bi 4*f* [part (b)], O 1*s* [part (c)], and Cu 2*p* [part (d)] core-level photoemission spectra using 1253.6-eV radiation for different Ag coverages (Θ).

TABLE II. Analysis of the intensity ratio (I_s/I_m) of the Cu 2*p*_{3/2} satellite to the Cu 2*p*_{3/2} main line for different Ag coverages (Θ).

Θ (Å)	I_s/I_m
0.0	0.5
1.1	0.4
2.5	0.3

and the near valence-band states (-7 eV to the Fermi level) is vastly diminished.

In contrast, both the Bi 4*f* and the O 1*s* core levels are more or less unaffected by the Ag overlayers, although the Bi 4*f* core levels exhibit a small shift towards lower binding energies by 0.1–0.2 eV for coverages beyond 2.5 Å. This inertness of both the Bi and the O states, which supposedly form the surface layer (see the discussion above), suggests that the surface of the $\text{Bi}_2\text{Sr}_2\text{CuO}_6$ material reacts only weakly with Ag adatoms.

The Cu 2*p* core level, however, shows evidence of reaction as is obvious from the monotonically decreasing intensity of the Cu 2*p* satellite for progressively thicker Ag overlayers. In fact, at a coverage of 5.3 Å the Cu 2*p* satellite is hardly visible. In Table II we summarize the intensity ratio of the Cu 2*p*_{3/2} satellite to the Cu 2*p*_{3/2} main line as a function of the Ag coverage. Thus, we conclude that the Cu valency—as reflected by the intensity ratio of the Cu 2*p*_{3/2} satellite to the Cu 2*p*_{3/2} main line—is extremely sensitive to the chemical environment. This finding is in agreement with the results of similar studies performed on polycrystalline and single-crystalline samples of the $\text{Bi}_2\text{Sr}_2\text{CaCu}_2\text{O}_8$ material that showed a clear reaction of the Cu 2*p* states without hardly any sign of reaction in the O 1*s* core-level data.^{14,15}

In short, the electronic structure of single-crystalline $\text{Bi}_2\text{Sr}_2\text{CuO}_6$ has been studied using ultraviolet and x-ray photoemission spectroscopy. The valence-band spectrum shows an overall agreement with the corresponding spectrum for single-crystalline $\text{Bi}_2\text{Sr}_2\text{CaCu}_2\text{O}_8$, although differences in the line shapes and strengths of the Sr 4*p*–O 2*s* semicore feature and the valence-band structures are observed. Both compounds exhibit a sharp Fermi-level cutoff, giving evidence of metallic character of $\text{Bi}_2\text{Sr}_2\text{CuO}_6$ and $\text{Bi}_2\text{Sr}_2\text{CaCu}_2\text{O}_8$ at room temperature. Also the core-level photoemission data show general agreement with the corresponding results for single-crystalline $\text{Bi}_2\text{Sr}_2\text{CaCu}_2\text{O}_8$; a single-component O 1*s* core level and a Cu 2*p* satellite to main line intensity ratio of about 0.5 are observed. An analysis of the relative core-level photoemission intensities shows good agreement with a theoretical model assuming a Bi–O terminated crystal, although the Sr and Cu signals are found to deviate somewhat from the theoretical predictions ($\sim 10\%$). Deposition of Ag onto the cleaved crystal shows that the Bi and O ions, which form the surface layer, are only weakly affected by the Ag adatoms, while the Cu 2*p* core-level spectra show evidence of reaction as the Cu valency is strong reduced.

ACKNOWLEDGMENTS

Two of the authors would like to thank AT&T (D.B.M.), and the Alfred P. Sloan Foundation and the National Science Foundation (A.K.) for support. This

work was supported by the U.S. National Science Foundation through the NSF-MRL program at the Center for Materials Research at Stanford University, Air Force Contract No. AFOSR-87-0389, and Joint Services Electronics Program Contract No. DAAG 29-85-K-0048.

-
- ¹See the review article of G. Wendin, *Physica Scr.* (to be published), and references therein.
- ²J. M. Tarascon, W. R. McKinnon, P. Barboux, D. M. Hwang, B. G. Bagley, L. H. Greene, G. Hull, Y. LePage, N. Stoffel, and M. Giroud, *Phys. Rev. B* **38**, 8885 (1988).
- ³D. B. Mitzi *et al.* (unpublished).
- ⁴Z.-X. Shen, P. A. P. Lindberg, P. Soukiassian, C. B. Eom, I. Lindau, W. E. Spicer, and T. H. Geballe, *Phys. Rev. B* **39**, 823 (1989).
- ⁵Z.-X. Shen, P. A. P. Lindberg, B. O. Wells, D. B. Mitzi, I. Lindau, W. E. Spicer, and A. Kapitulnik, *Phys. Rev. B* **38**, 11 820 (1988).
- ⁶H. M. Meyer III, D. M. Hill, J. H. Weaver, D. L. Nelson, and C. F. Gallo, *Phys. Rev. B* **38**, 7144 (1988).
- ⁷A. Fujimori, S. Takekawa, E. Takayama-Muromachi, Y. Uchida, A. Ono, T. Takahashi, Y. Okabe, and H. Katayama-Yoshida, *Phys. Rev. B* **39**, 2255 (1989).
- ⁸P. Steiner, S. Hüfner, A. Jungmann, S. Junk, V. Kinsinger, I. Scuder, W. R. Thiele, N. Backer, and C. Politis, *Physica C* **156**, 213 (1988).
- ⁹P. A. P. Lindberg, I. Lindau, and W. E. Spicer, *Phys. Rev. B* **40**, 6822 (1989).
- ¹⁰P. A. P. Lindberg, Z.-X. Shen, B. O. Wells, D. S. Dessau, D. B. Mitzi, I. Lindau, W. E. Spicer, and A. Kapitulnik, *Phys. Rev. B* **39**, 2890 (1989).
- ¹¹P. A. P. Lindberg, Z.-X. Shen, B. O. Wells, D. B. Mitzi, I. Lindau, W. E. Spicer, and A. Kapitulnik, *Appl. Phys. Lett.* **53**, 2563 (1988).
- ¹²M. D. Kirk, J. Nogami, A. A. Baski, D. B. Mitzi, A. Kapitulnik, T. H. Geballe, and C. F. Quate, *Science* **242**, 1673 (1988).
- ¹³M. D. Kirk, C. B. Eom, B. Oh, S. R. Spielman, M. R. Beasley, A. Kapitulnik, T. H. Geballe, and C. F. Quate, *Appl. Phys. Lett.* **52**, 2076 (1988).
- ¹⁴P. A. P. Lindberg, Z.-X. Shen, I. Lindau, W. E. Spicer, C. B. Eom, and T. H. Geballe, *Appl. Phys. Lett.* **53**, 529 (1988).
- ¹⁵H. M. Meyer III, D. M. Hill, T. J. Wagener, J. H. Weaver, C. F. Gallo, and K. C. Goretta, *J. Appl. Phys.* **65**, 3130 (1989).